Published in final edited form as:
Dev Biol. 2014 June 15; 390(2): 149–159. doi:10.1016/j.ydbio.2014.03.015.

CEH-28 activates *dbl-1* expression and TGF-ß signaling in the *C. elegans* M4 neuron

Kalpana Ramakrishnan[1], **Paramita Ray**[1,2], and **Peter G. Okkema**[1,2,3]

[1]Department of Biological Sciences, University of Illinois at Chicago, 900 S. Ashland Avenue (MC567), Chicago, IL 60607, USA

Abstract

M4 is a multifunctional neuron in the *C. elegans* pharynx that can both stimulate peristaltic contractions of the muscles in the pharyngeal isthmus and function systemically to regulate an enhanced sensory response under hypoxic conditions. Here we identify a third function for M4 that depends on activation of the TGF-ß family gene *dbl-1* by the homeodomain transcription factor CEH-28. *dbl-1* is expressed in M4 and a subset of other neurons, and we show CEH-28 specifically activates *dbl-1* expression in M4. Characterization of the *dbl-1* promoter indicates that CEH-28 targets an M4-specific enhancer within the *dbl-1* promoter region, while expression in other neurons is mediated by separate regulatory sequences. Unlike *ceh-28* mutants, *dbl-1* mutants do not exhibit M4 synaptic and signaling defects. Instead, both *ceh-28* and *dbl-1* mutants exhibit morphological defects in the g1 gland cells located adjacent to M4 in the pharynx, and these defects can be partially rescued by M4-specific expression of *dbl-1* in these mutants. Identical gland cell defects are observed in *sma-6* and *daf-4* mutants defective in the receptor for DBL-1, but they are not observed in *sma-2* and *sma-3* mutants lacking the R-Smads functioning downstream of this receptor. Together these results identify a novel neuroendocrine function for M4 and provide evidence for an R-Smad-independent mechanism for DBL-1 signaling in *C. elegans*.

Keywords

C. elegans; pharynx; TGF-ß signaling; gland cells; motor neuron; R-Smad independent

Introduction

At the cellular level, the *C. elegans* nervous system is remarkably simple and well characterized. In adult hermaphrodites, the nervous system consists of 302 cells that can be

[3]Corresponding author: Peter Okkema, Department of Biological Sciences, University of Illinois at Chicago, 900 S. Ashland Avenue (MC567), Chicago, IL 60607, USA, okkema@uic.edu, tel. 1-312-413-7445, fax 1-312-413-2691 .
[2]Current address: Department of Radiation Oncology, University of Michigan, Ann Arbor, MI 48109 USA

divided into a pharyngeal nervous system of 20 cells and an extra-pharyngeal nervous system of 282 cells. Electron micrographic reconstructions have produced a wiring diagram describing cellular morphology and synaptic connectivity throughout both the pharyngeal and extra-pharyngeal nervous systems (Albertson and Thomson, 1976; White et al., 1986). While many excellent studies have revealed a great deal about how this nervous system senses the environment, controls various behaviors, and affects development (Ardiel and Rankin, 2010; Avery and You, 2012; Schafer, 2005), we still do not understand how such a simple nervous system carries out so many complex functions.

Many *C. elegans* neurons appear multifunctional and cannot be easily classified as a single morphological type, such as motor neuron, sensory neuron, or interneuron (Albertson and Thomson, 1976; White et al., 1986). In addition, a variety of neurons also synthesize factors controlling developmental and homeostatic processes such as dauer formation, fat storage, and body size (Ashrafi, 2007; Gumienny and Savage-Dunn, 2013; Hu, 2007). Such multifunctionality may be one mechanism by which this simple nervous system controls many complex behaviors (Avery and Thomas, 1997).

The pharyngeal motor neuron M4 is a multifunctional neuron that stimulates contraction of the muscles in a region of the pharynx called the isthmus and regulates enhanced sensory perception during hypoxia (Avery and Horvitz, 1989; Pocock and Hobert, 2010). M4 forms *en passant* synapses on the muscles in the posterior isthmus, and synaptic vesicles at these synapses are believed to release acetylcholine onto the isthmus muscles to stimulate a wave-like, peristaltic contraction in these muscles (Albertson and Thomson, 1976; Ray et al., 2008). M4 also contains larger dense core vesicles (DCVs) that are not found in other pharyngeal motor neurons (Albertson and Thomson, 1976). DCVs are believed to secrete neuropeptides and hormones (Burgoyne and Morgan, 2003), and the M4 DCVs likely release the FMRFamide neurotransmitter FLP-21 to affect the extra-pharyngeal nervous system under hypoxic conditions (Pocock and Hobert, 2010). In addition, both morphological features and gene expression patterns suggest M4 has other signaling functions. First M4 synapses onto the pharyngeal g1 gland cells, which are secretory cells that extend ducts through the isthmus that join the pharyngeal lumen (Albertson and Thomson, 1976). The gland cells secrete a variety of mucin-like proteins that facilitate bacterial transport through the pharyngeal lumen during feeding (Smit et al., 2008). Second, M4 expresses genes encoding signaling molecules such as the FGF-family member *egl-17* and the TGF-ß family member *dbl-1* suggesting M4 may have other signaling functions (Burdine et al., 1998; Suzuki et al., 1999).

We are interested in the role the NK-2 homeodomain transcription factor CEH-28 plays in M4. CEH-28 is expressed exclusively in M4 from mid-embryogenesis through adulthood, and it plays a crucial role in regulating M4 synapse formation and stimulation of isthmus peristalsis (Ray et al., 2008). In *ceh-28* mutants, synapses are morphologically abnormal, and they are inappropriately located in regions that normally exhibit dendritic characteristics (Albertson and Thomson, 1976). *ceh-28* mutants can hyper-stimulate peristaltic contractions of the pm5 muscles that make up the pharyngeal isthmus (Ray et al., 2008).

In this work we investigate the function and regulation of *dbl-1* gene expression in M4. *dbl-1* encodes a TGF-ß family factor that is part of the Sma/Mab pathway, and it is expressed in M4 and a subset of pharyngeal and extra-pharyngeal neurons (Gumienny and Savage-Dunn, 2013). *dbl-1* was initially characterized based on its developmental role as a regulator of body size and male tail morphogenesis (Morita et al., 1999; Suzuki et al., 1999), but more recently it has been found to function throughout the life-cycle as a regulator of innate immunity, reproductive aging, and aversive olfactory learning (Luo et al., 2010; Zhang and Zhang, 2012; Zugasti and Ewbank, 2009).

Here we show that *dbl-1* expression in M4 depends on CEH-28, and that *dbl-1* expression in M4 regulates g1 gland cell morphology. CEH-28 activates *dbl-1* expression in M4 by targeting a cell-specific enhancer, and mutation of CEH-28 binding sites in this enhancer strongly reduces its activity. The g1 gland cells exhibit abnormal morphology in both *ceh-28* and *dbl-1* mutants, and restoring expression of *dbl-1* in M4 partially rescues these mutant defects. DBL-1 secretion does not depend on DCV release as *unc-31* mutants defective in this process exhibit normal gland cell morphology. DBL-1 signaling affecting gland cells requires the Sma/Mab pathway receptors SMA-6 and DAF-4 but does not require the receptor-regulated Smads SMA-2 and SMA-3. These results identify a novel function for DBL-1 and the M4 cell, and we suggest DBL-1 protein secreted from M4 non-autonomously activates a Smad-independent TGF-ß signaling pathway affecting gland cell morphology.

Materials and Methods

Nematode handling, transformation and strains

C. elegans were grown under standard conditions (Lewis and Fleming, 1995). Germline transformations were performed using standard techniques (Mello and Fire, 1995) using injection mixes containing pRF4 *rol-6(su1006)* (100 ng/µl) and *gfp* or other plasmids (10-25 ng/µl).

The following strains were used in this study: BW1946 *ctIs43[Pdbl-1::gfp]; unc-42(e270) V*, BW1806 *dbl-1(ev580*) *V* (kindly provided by Y. Suzuki, University of Colorado), (Suzuki et al., 1999), OK0542 *ctIs43; unc-42(e270) V; ceh-28(cu11*) *X*, OK0543 *ctIs43; unc-42(e270) V; ceh-28(tm1258) X*, OK0435 *cuEx324[ceh-28::gfp]* (Ray et al., 2008), OK0545 *dbl-1(ev580); cuEx324*

The following strains were used to analyze 5′ deletions of the *dbl-1* promoter: OK0830 *cuEx659[Pdbl-1::gfp −3764Δ]*, OK0833 *cuEx662[Pdbl-1::gfp −3061Δ]*, OK0837 *cuEx666[Pdbl-1::gfp* -2472Δ*]*, OK0839 *cuEx668[Pdbl-1::gfp −1278Δ];* OK0842 *cuEx671[Pdbl-1::gfp −646Δ]*

The following strains were used to assay *dbl-1* M4 enhancer activity in wild-type and *ceh-28(cu11*) mutants respectively: OK0765 *cuEx613[dbl-1 M4 enhancer*$^{wild\text{-}type}$*]*, OK0766 *ceh-28(cu11); cuEx613*, OK0772 *cuEx619[M4 enhancer*$^{-825mut}$*]*, OK0774 *cuEx621[M4 enhancer*$^{-738mut}$*]*, OK0780 *cuEx627[M4 enhancer*$^{double\_mut}$*]*

The following strains were used to examine pharyngeal g1 gland cell morphology GD26 *ivEx[phat-3::yfp]* (kindly provided by J. Gaudet, University of Calgary), OK0567 *ceh-28(cu11); ivEx[phat-3::yfp],* OK571 *ceh-28(tm1258); ivEx[phat-3::yfp],* OK0792 *dbl-1(ev580); phat-3::yfp,* OK585 *daf-1(m40) IV; ivEx[phat-3::yfp],* OK586 *daf-4(m72)III; ivEx[phat-3::yfp],* OK584 *sma-6(wk7); ivEx[phat-3::yfp],* OK0977 *ivIs12[phat-1::yfp*] (kindly provided by J. Gaudet, University of Calgary, Canada), GD273 *sma-2(e502) III; ivIs12 II,* GD274 *sma-3(e491) III; ivIs12 II* (Raharjo et al., 2011), OK1014 *daf-8(e1393) I; ivIs12 II,* OK1015 *daf-14(m77) IV; ivIs12 II,* OK1016 *daf-3(mg90) X; ivEx[phat-3::yfp],* OK1017 *sma-4(e729) III; ivIs12 II,* OK0762 *cuEx611[pser-7b::dbl-1; phat-3::yfp],* OK0763 dbl-1(ev580); cuEx611, OK0859 ceh-28(cu11); cuEx611. N2 worms were injected with 15 ng/μl of pOK210.01 *[phat-3::yfp],* pOK230.01*[Pser-7b::dbl-1]* and 100 ng/μl of pRF4 to make OK0762.

To investigate gland morphology in *unc-31* mutants, the following strains were used, CB928 *unc-31(e928)* (kindly provided by J. Richmond, UIC), and OK0973 *unc-31(e928); ivIs12*.

General methods for nucleic acid manipulations and plasmid construction

Standard methods were used to manipulate all DNA sequences (Ausubel, 1990) and all plasmids are available from the authors.

The full-length *Pdbl-1::gfp* pMY+NLS/pOK205.01 containing bp 11,900-16,530 of T25F10 cosmid (Accession #U64856) was provided by W. Wood (University of Colorado) (Suzuki et al., 1999). Deletions in *Pdbl-1::gfp* are named to indicate the number of base-pairs upstream of the *dbl-1* translational start site and were generated by restriction digestion to the following sites in the *dbl-1* promoter: SphI (−3764Δ; pOK264.09), NheI (−3601Δ; pOK264.01), DraIII (−2472Δ; pOK264.03), HindIII (−1278Δ; pOK 264.07), and XbaI (−646Δ; pOK264.05).

The M4 enhancer$^{\text{wild-type}}$ was amplified from pOK205.01, and a HindIII-XbaI fragment (bp 15,281-15,916 of cosmid T25F10) was inserted upstream of the Δ*pes-10::gfp* to make pOK272.06. CEH-28 binding sites in the enhancer where separately mutated using Quik Change Lightning Multi Kit (Stratagene) in pOK272.06 to produce M4 enhancer$^{-825\text{mut}}$ plasmid pOK277.01 and M4 enhancer$^{-738\text{mut}}$ plasmid pOK277.03, respectively. The M4 enhancer$^{\text{double_mut}}$ plasmid pOK277.05 was created by mutating the site at −738bp in pOK277.01. The constructs were sequenced to confirm the presence of targeted mutations. The adjacent fragment of the *dbl-1* promoter (bp 13,502-15,284 of cosmid T25F10) was amplified and a HindIII-NheI was inserted upstream of Δ*pes-10::gfp* to generate pOK274.19.

The *Pser-7b::dbl-1* expression plasmid pOK230.01 was constructed by amplifying the full-length *dbl-1* orf from yk1350b03/pOK227.03 (provided by Y. Kohara) with primers PO801 [AGGTACCAAAATGAACGACTCTGTGCGGAC] and PO803 [CCAGAATTCTAATGTGCGACGACGATGG] digesting with KpnI and EcoRI, and inserting this fragment downstream of the *ser-7b* promoter in KpnI-EcoRI digested pOK197.03 (Hobson et al., 2003).

Identification of candidate CEH-28 binding sites in the *dbl-1* promoter

Candidate CEH-28 binding sites were identified by scanning the *dbl-1* promoter using the WormBase function Annotate Sequence Motif (www.wormbase.org) with the JASPAR position-frequency-matrix MA0264.1 (jaspar.cgb.ki.se) at a threshold of 0.82 (Berger et al., 2006). We identified 8 CEH-28 binding sites starting at base pair −2810, −2668, −2441, −2107, −2042, −835, −738, and −497 bp upstream of the *dbl-1* translational start site. Conserved sites were identified in the *dbl-1* promoter using multiz alignments of the *C. elegans, C. briggsae, C. remanei, C. brenneri* and *C. sp. 11* genomes (http://genome.ucsc.edu/).

Microscopy

Micrographs of wild-type and mutant animals were acquired using a Zeiss Axioskop microscope using an Axiocam MRm camera. Images were analyzed using AxioVision software and processed using Adobe Photoshop.

To analyze pharyngeal pumping and peristalsis, L1 larvae from wild-type and *dbl-1(ev580)* were selected and recorded as described previously (Ray et al., 2008). For each genotype, pumping and peristalsis were analyzed in at least 5 animals for approximately 30 seconds.

M4 synapses in wild-type and *dbl-1(ev580)* mutants were visualized using a *ser-7b::snb-1::gfp* fusion described previously (Ray et al., 2008). Z-stacks of SNB-1::GFP were acquired using a Zeiss Axiovert 200 microscope and deconvolved using AxioVision 4.3 software. Adjacent focal planes exhibiting GFP throughout two pharyngeal nerve cords were Z-projected using maximum fluorescence and fluorescence intensity profiles were generated on a Macintosh computer using ImageJ (developed at the US NIH and available at http://rsb.info.nih.gov/nih-image/).

Results

dbl-1::gfp is not expressed in *ceh-28* mutant M4 cells

A *dbl-1* promoter::*gfp* fusion (*Pdbl-1::gfp*) containing a 4.6 kb promoter fragment was previously shown to be expressed in a subset of neurons, including the pharyngeal neurons M1, M2, M4, M5 and I5, as well as non-pharyngeal neurons including some amphid neurons and neurons of the ventral nerve cord (Suzuki et al., 1999). To determine if *dbl-1* expression in M4 requires CEH-28, we compared expression of *Pdbl-1::gfp* in wild-type animals and *ceh-28* mutants. In wild-type animals, strong *Pdbl-1::gfp* expression was observed in the M4 cell in 96% of transgenic adults (Figure 1 B,C; n=57). In comparison, strong *Pdbl-1::gfp* expression in M4 was observed in only 17% of *ceh-28(cu11)* adults (n=53) (Figure 1 D,E) and 19% of *ceh-28(tm1258)* adults (n=47). Thus, *ceh-28* functions upstream of *dbl-1* and is specifically required for *Pdbl-1::gfp* expression in M4. A *ceh-28::gfp* reporter is expressed normally in the M4 neuron of *dbl-1(ev580)* mutants (Supplementary Figure 1), indicating that DBL-1 is not necessary for M4 differentiation.

The *dbl-1* promoter contains separable regulatory regions controlling expression in M4 and other neurons

To determine if the *dbl-1* promoter could be directly targeted by CEH-28, we searched for sequences matching the binding site for the related NK-2 homeodomain factor CEH-22 (jaspar.genereg.net; ID MA0264.1; (Berger et al., 2006)). NK-2 family factors are characterized by a tyrosine residue at homeodomain position 54 that is crucial to DNA-binding specificity (Harvey, 1996; Pradhan et al., 2012), and CEH-22 and all characterized members of this family bind similar DNA sites (Berger et al., 2006; Okkema and Fire, 1994). The CEH-22 and CEH-28 homeodomains are 62% identical, and it is likely they exhibit very similar DNA-binding specificity. We found 8 candidate CEH-28 binding sites in the *dbl-1* promoter (Figure 2A), with three of these sites conserved in the *dbl-1* promoter in related nematodes based on multiz alignments (http://genome.ucsc.edu/).

To identify sequences regulating *dbl-1* expression, we examined the intensity and frequency of GFP expression in transgenic animals bearing 5′-deletions of *Pdbl-1::gfp*. Notably, a deletion to −2472 largely eliminated *Pdbl-1::gfp* expression in most neurons but retained strong expression in M4 (Figure 2A,D; Table 1). This suggests separable regulatory sequences control *dbl-1* expression in M4 and other neurons. A moderate decrease in the frequency and intensity of *Pdbl-1::gfp* expression was observed when sequences were further deleted to −1278, and expression was completely lost when deleted to −646 (Figure 2 E,F; Table 1). These results suggest that the candidate CEH-28 binding sites in the *dbl-1* promoter contribute additively to expression in M4, and indicate that the region between −1278 to −646 contains sequences necessary for activating *dbl-1* expression in M4.

The *dbl-1* promoter contains an M4-specific enhancer activated by CEH-28

We next tested fragments of the *dbl-1* promoter containing candidate CEH-28 binding sites for enhancer activity by asking if they could activate expression of a Δ*pes-10::gfp* reporter. The Δ*pes-10::gfp* alone is not expressed in transgenic *C. elegans*, but it is sensitive to upstream enhancers (Okkema and Fire, 1994). A 1783 bp fragment between regions −3061 bp to −1278 bp containing 5 candidate CEH-28 binding sites had no detectable enhancer activity (Figure 3A; data not shown). In contrast, the adjacent 632 bp fragment between regions −1278 bp to −646 bp containing 2 candidate CEH-28 sites exhibited strong, M4-specific enhancer activity, and we refer to this fragment as the M4 enhancer (Figure 3 A,B; Table 2). When examined in a *ceh-28(cu11)* null mutant background, activity of the M4 enhancer was completely lost (Figure 3C; Table 2). Thus the M4 enhancer depends on CEH-28.

The M4 enhancer contains two candidate CEH-28 binding sites: one located at bp −825, which is conserved in other *Caenorhabditis* species, and a second at bp −738. We tested the effect of mutations in each of these sites on M4 enhancer activity either alone or in a double mutant. Mutation of the site at −825 led to a decrease in the intensity of GFP expression level and a moderate decrease in the frequency of animals expressing GFP, whereas mutation of the site at −738 had little effect on enhancer activity (Figure 3D, E; Table 2). In comparison, a double mutant affecting both of these sites had a stronger reduction in both the intensity and frequency of GFP expression in M4, although weak expression was still

observed in some animals (Figure 3F; Table 2). These results indicate that both sites contribute to activity of the M4 enhancer, and strongly suggest that CEH-28 directly activates *dbl-1* expression in M4.

M4 neuronal function and synapses are normal in *dbl-1* mutants

ceh-28 mutants exhibit frequent and prolonged peristalses of the pharyngeal isthmus muscles and a stuffed pharynx phenotype, and we believe these phenotypes result from abnormal and mispositioned synapses in M4 throughout the isthmus (Ray et al., 2008). Because, TGF-ß mediated signals have been implicated in synapse assembly and positioning in other organisms (Marques, 2005), we examined M4 neuronal function and synapses in *dbl-1(ev580)* mutants. However, in both assays, *dbl-1* mutants appear normal.

We used video microscopy to examine pharyngeal contractions in wild-type and *dbl-1(ev580)* mutant L1 larvae, and found *dbl-1* mutants exhibit normal pharyngeal pumping and peristalses. In particular, the length of isthmus peristalses are very similar in wild type and *dbl-1* mutants (Table 3). Consistent with normal pharyngeal function, we never observed a stuffed pharynx phenotype in *dbl-1(ev580)* mutant adults (n=74).

We next examined synapses in *dbl-1(ev580)* mutants using a *snb-1::gfp* fusion gene expressed specifically in the M4 cell using the *ser-7b* promoter (Ray et al., 2008). SNB-1::GFP is a functional synaptobrevin that marks synaptic vesicles (Nonet, 1999). In both wild-type and *dbl-1(ev580)* animals SNB-1::GFP marked synapses are appropriately localized in the posterior region of the pharyngeal isthmus and these synapses appear more uniformly sized and spaced than we have previously observed in *ceh-28* mutants (Figure 4) (Ray et al., 2008).

In summary, the M4 cell function and synaptic morphology in *dbl-1(ev580)* mutants appears similar to that of wild-type animals. These observations are in sharp contrast with those from similar analyses of *ceh-28* mutants (Ray et al., 2008), and they indicate *dbl-1* is not necessary for M4 synapse formation or neuronal function.

ceh-28 and *dbl-1* mutants exhibit similar defects in pharyngeal g1 gland cell morphology

The function of DBL-1 in M4 is unknown, but, as a secreted growth factor, it likely affects nearby cells. The g1 pharyngeal gland cells are in close proximity to M4, and M4 forms synapses on g1 (Albertson and Thomson, 1976). The g1 cell bodies are located in the posterior bulb of the pharynx, and they extend processes anteriorly along the dorsal and subventral pharyngeal nerve cords, where they contact the M4 neuronal processes (Figure 5A). The dorsal process extends the length of the pharynx and connects to the pharyngeal lumen near the anterior tip of the pharynx, whereas the subventral processes extend through the isthmus and connect to the lumen near the anterior bulb.

We examined the g1 gland cells in *ceh-28* and *dbl-1* mutants and found these animals had nearly identical defects in gland cell morphology. The g1 gland cells were visualized using *phat-3::yfp* and *phat-1::yfp* reporters labeling the g1 gland cell bodies and processes (kindly provided by J. Gaudet), and identical results were obtained using *hlh-6::gfp* and *kel-1::gfp* reporters as markers (data not shown). In wild-type animals, the gland cell processes are thin

and have a uniform diameter along their entire length (Figure 5B). In comparison, we found these processes in the mutants often appeared thicker than in wild-type animals and often exhibited abnormal swellings near the M4 cell body (Figure 5C-E). To rule out the possibility that gland cell defects result from the reporter genes themselves, we directly compared wild type and *ceh-28(cu11)* mutant gland cell processes in non-transgenic animals using DIC microscopy and found that *ceh-28(cu11)* mutants had g1 gland cell processes that were wider than those in wild-type animals (Figure 6). While the *ceh-28(cu11)* gland cell processes contained vesicles similar to those of wild type animals, these processes did not appear stuffed with vesicles, as has been previously observed in *daf-9* and *peb-1* mutants that also exhibit enlarged gland cell processes (Albert and Riddle, 1988; Fernandez et al., 2004).

Normal gland cell morphology depends on the SMA-6 and DAF-4 receptors but is independent of R-Smads

DBL-1 is a TGF-ß family ligand that is known to regulate body size and male tail morphogenesis through the Sma/Mab signaling pathway (Gumienny and Savage-Dunn, 2013), and we asked if other components of this pathway also affect gland cell morphology. *sma-6* and *daf-4* encode Type I and Type II receptor subunits, respectively, that bind DBL-1, and we find that both *sma-6* and *daf-4* mutants exhibit g1 gland cell abnormalities similar to those observed in *dbl-1* mutants (Figure 5F,G, Table 4).

DAF-4 also functions in another TGF-ß signaling pathway regulating dauer larvae formation with the DAF-1 Type I receptor subunit (Gumienny and Savage-Dunn, 2013), and we asked if this pathway also regulates gland cell morphology. We found that *daf-1* mutants exhibit only a weak gland cell defect, and most *daf-1* mutants have a normal g1 gland cell morphology (Figure 5H, Table 4).

Downstream signaling in response to TGF-ß receptor activation can occur via either Smad-dependent or Smad-independent pathways (Sieber et al., 2009). *sma*-2 and *sma-3* encode R-Smads that function in the Sma/Mab pathway, while *sma-4* encodes a co-Smad in this pathway (Gumienny and Savage-Dunn, 2013). *sma-2* and *sma-3* mutants were previously shown to have normal g1 gland cells (Raharjo et al., 2011), and we made similar observations (Figure 5I,J, Table 4). *sma-4* mutants exhibited g1 gland cell defects at a low frequency comparable to those observed in *daf-1* mutants, but most *sma-4* animals had a normal gland cell morphology (Table 4; Figure 5K; Supplementary Figure 2). *daf-8* and *daf-14* encode R-Smads that function in the dauer formation pathway, while *daf-3* encodes the co-Smad in this pathway (Gumienny and Savage-Dunn, 2013), and mutants affecting each of these genes exhibited normal gland cell morphology (Table 4; Supplementary Figure 2). Thus DBL-1 affects gland cell morphology independently of the known R-Smads and functions through a Smad-independent signaling pathway mediated by the SMA-6 and DAF-4 receptors.

dbl-1 expression in M4 partially rescues gland cell defects in *ceh-28* and *dbl-1* mutants

We hypothesize that DBL-1 is expressed and secreted from M4 to affect gland cell morphology. To test this hypothesis, we asked if expressing *dbl-1* in the M4 cell using the

ser-7b promoter would rescue gland cell defects of *dbl-1* and *ceh-28* mutants. The *ser-7b* promoter is active exclusively in M4, and we have previously shown it remains active in *ceh-28* mutants (Hobson et al., 2003; Ray et al., 2008). Wild-type animals bearing this transgene exhibited normal gland cell morphology, indicating that *ser-7b::dbl-1* expression did not adversely affect gland cell morphology (Figure 7A; Table 4).

ser-7b::dbl-1 partially rescued gland cell defects in both *dbl-1* and *ceh-28* mutants (Figure 7 B,C; Table 4), although some animals still exhibited gland cell abnormalities. These results indicate *dbl-1* expression in M4 does affect gland cell morphology. Because both the *dbl-1* mutants lacking all DBL-1 activity and *ceh*-28 mutants lacking DBL-1 only in M4 exhibited similar levels of rescue, we conclude that M4 is the major source of DBL-1 affecting gland cell morphology.

DBL-1 secretion from M4 is not mediated by dense core vesicles

Neurons use dense core vesicles (DCVs) to secrete neuropeptides and proteins from their cell somas using the regulated pathway of secretion (Burgoyne and Morgan, 2003). The M4 neuron contains dense core vesicles, and these DCVs are likely involved in secreting the FLP-21 peptide that controls feeding behavior under hypoxic conditions (Albertson and Thomson, 1976; Pocock and Hobert, 2010). DCVs have been previously implicated in secreting TGF-ßs in mammals (Krieglstein and Unsicker, 1995; Lacmann et al., 2007; Specht et al., 2003), and we were interested in determining if DBL-1 secretion from M4 might be similarly mediated by DCVs.

unc-31 encodes the only form of the calcium-activated protein for secretion (CAPS) in *C. elegans*, and it is specifically required for DCV release (Sieburth et al., 2007; Speese et al., 2007). To investigate if DBL-1 secretion from M4 to the gland cells is mediated by DCVs, we visualized g1 gland cell morphology in *unc-31(e928)* null mutants using a *phat-1::yfp* gland cell reporter. However, none of the mutants exhibited gland cell abnormalities (Supplementary Figure 3; n=35). This result indicates DCV release is not necessary for DBL-1 secretion from M4 via the regulated pathway and suggests that DBL-1 secretion is mediated by other secretory mechanisms.

Discussion

Here we show that the NK-2 homeodomain transcription factor CEH-28 functions specifically in M4 and regulates a previously unidentified neurosecretory function of M4 by activating the TGF-ß family gene *dbl-1*. The *dbl-1* promoter contains largely separable sequences activating *dbl-1* expression in M4 and other neurons, and CEH-28 directly targets an M4 specific enhancer within the *dbl-1* promoter. *dbl-1* expression in M4 affects morphology of the g1 gland cells, which directly contact M4. Despite being enriched in DCVs, M4 does not require DCV secretion to affect the gland cells, suggesting that DBL-1 is secreted through the constitutive exocytic pathway rather than through regulated release of DCVs (reviewed in (Burgoyne and Morgan, 2003)). Finally we demonstrate that DBL-1 affects gland cells through a Smad-independent, non-canonical TGF-ß signaling pathway (reviewed in (Zhang, 2009)).

CEH-28 is an upstream regulator of TGF-ß signaling in M4

Our results strongly suggest that CEH-28 directly activates *dbl-1* expression in M4. The *dbl-1* promoter contains separate regions that control expression in M4 and other neurons, and we identified a transcriptional enhancer that specifically activates transcription in the M4 cell. Activity of this enhancer was completely dependent on wild-type CEH-28, and mutation of two candidate CEH-28 binding sites strongly reduced enhancer activity. These CEH-28 binding sites appear partially redundant, as single mutants retain more enhancer activity than the double mutant. Interestingly, the site at −825 has the strongest affect on enhancer activity and this site is conserved in Multiz alignments of the *C. elegans, C. briggsae, C. remanei, C. brenneri* and *C. sp. 11* genomes (Kent et al., 2002). In comparison, the site at −738 is not conserved at this position in alignments with other species, and mutation of this site affects enhancer activity only when both it and the −825 site are mutated. The observation that enhancer activity is lost in *ceh-28* mutants, while low level enhancer activity remains when these binding sites are mutated suggests additional sequences contribute to enhancer activity in M4. These sequences might contain more highly diverged CEH-28 binding sites, or alternatively a site for another transcription factor that is dependent on CEH-28.

In mammals, the CEH-28-related factor NKX2.1 directly activates expression of the TGF-ß family gene *Bmp4* in lung epithelial cells (Zhu et al., 2004), suggesting that TGF-ß family gene regulation by NK-2 homeodomain factors is conserved in some contexts. In the developing mouse lung, *Nkx2.1* and *Bmp4* are co-expressed only in the distal branching epithelium (Zhu et al., 2004), and decreased activity of either Nkx2.1 or Bmp4 results in similar defects in distal lung morphogenesis (Minoo et al., 1999; Weaver et al., 1999). While the processes of the pharyngeal gland cells in *C. elegans* are structurally very different than branching epithelia in the lung, it is tempting to speculate that TGF-ß family gene regulation may have a conserved function in morphogenesis of tubular structures.

Analysis of gland cell morphology in *ceh-28* and *dbl-1* mutants reveals a new function for M4

M4 has two previously recognized functions. Ultrastructural and functional studies demonstrated M4 functions as a motor neuron to stimulate peristaltic contraction of the muscles in the isthmus of the pharynx (Albertson and Thomson, 1976; Avery and Horvitz, 1989), and this function likely depends on the release of acetylcholine from M4 (Ray et al., 2008). More recently, a second function of M4 was described in an enhanced sensory response under hypoxic conditions (Pocock and Hobert, 2010), and this function depends on release of the FMRFamide related neuropeptide FLP-21.

In this work, we describe a third function for M4 in which secretion of the TGF-ß family factor DBL-1 affects the morphology of the g1 gland cells. *ceh-28* mutants and *dbl-1* mutants exhibit abnormal gland cell morphology that include thicker processes and swellings near the M4 cell body. It is unlikely that the gland cells are enlarged due to increased secretion of gland cell-specific mucin-like proteins because the *phat* genes encoding these proteins are not over expressed in *dbl-1* mutants (Ghai and Gaudet, 2008; Roberts et al., 2010). Likewise the *dbl-1* mutant gland cell processes are not filled with

vesicles as has been observed in *daf-9* and *peb-1* mutants, which have enlarged gland cells resulting from molting defects (Albert and Riddle, 1988; Fernandez et al., 2004; Jia et al., 2002). g1 gland cell secretory activity is increased prior to molting, and these secretions are believed to aid in shedding the cuticle lining the pharynx (Hall and Hedgecock, 1991). However, neither *ceh-28* nor *dbl-1* mutants have any obvious molting defects, suggesting *dbl-1* expression in M4 does not stimulate this pre-molt secretory activity.

Our data indicates that M4 is the major source of DBL-1 signal that affects gland cell morphology. However it is not clear whether DBL-1 secreted from M4 affects the gland cells directly, or whether its effect could be indirect. M4 forms synapses on the g1 gland cells, and these synapses have been suggested to stimulate gland cell activity during molting and feeding (Albertson and Thomson, 1976). However, DBL-1 secreted from M4 could also indirectly affect gland cell morphology by altering the integrity of the pharyngeal muscle cells that surround the gland cell processes. Both M4 and the g1 gland cell processes contact pharyngeal muscles in the isthmus, and mutants that have weakened pharyngeal muscles exhibit abnormalities in gland cell morphology similar to those we observe in *ceh-28* and *dbl-1* mutants (Albertson and Thomson, 1976; Raharjo et al., 2011). The pharyngeal muscles have been shown to express the receptor protein SMA-6, while expression has not yet been reported in the gland cells (Krishna et al., 1999; Yoshida et al., 2001).

DBL-1 affects gland cell morphology through an R-Smad independent pathway

Many characterized effects of TGF-ß signaling depend on the canonical TGF-ß signaling pathway in which activated receptors phosphorylate receptor regulated Smads (R-Smads), leading to complex formation with a co-Smad and translocation into the nucleus (Sieber et al., 2009). More recently, a number of noncanonical, Smad-independent responses to TGF-ß signaling have been identified in which activated receptors instead target other signaling pathways, including branches of the MAPK, PI3K-Akt, RhoA-like small GTPase pathways (reviewed in (Mu et al., 2012; Zhang, 2009)).

Both canonical and noncanonical responses to DBL-1 have been described in *C. elegans* (reviewed in (Gumienny and Savage-Dunn, 2013)). DBL-1 functions through the canonical Sma/Mab pathway and depends on the R-Smads SMA-2 and SMA-3 to regulate body size, male tail morphogenesis and aversive olfactory learning (Savage et al., 1996; Zhang and Zhang, 2012). In contrast, a noncanonical pathway that only requires SMA-3 mediates DBL-1 regulation of innate immunity (Zugasti and Ewbank, 2009).

Here we show that DBL-1 affects gland cell morphology independently of both the Sma/Mab pathway R-Smads SMA-2 and SMA-3, as well as the dauer formation pathway R-Smads DAF-8 and DAF-14. These observations are consistent with results of previous studies examining gland cell morphology in mutants with small body size (Raharjo et al., 2011). While we do see a minor role for the co-Smad SMA-4 in affecting gland cells, this work suggests a R-Smad independent pathway for DBL-1 signaling through the SMA-6 and DAF-4 receptors exists in *C. elegans*, and this pathway plays a key role in M4 regulation of gland cell morphology.

Dense core vesicle release is not necessary for DBL-1 secretion from M4

M4 is unique among pharyngeal neurons in that it contains dense core vesicles (Albertson and Thomson, 1976), and neuronal DCVs are often associated with neuropeptide secretion (Burgoyne and Morgan, 2003). DCVs have also been shown to mediate regulated secretion of TGF-ß family ligands in chromaffin and PC12 cells (Krieglstein and Unsicker, 1995; Specht et al., 2003), and activity-dependent TGF-ß secretion affecting synaptic plasticity in hippocampal neurons (Lacmann et al., 2007). Active movement of vesicles is visible in the g1 gland cell ducts prior to molting and during feeding (Albertson and Thomson, 1976; Hall and Hedgecock, 1991), and this activity could in principle be controlled by regulated secretion of DBL-1 from M4 via DCVs. However, our results indicate DBL-1 is secreted from M4 independently of DCVs, as *unc-31* null mutants lacking DCV secretion exhibit normal gland cell morphology. These results suggest that DBL-1 is secreted through the constitutive secretory pathway, rather than through regulated release of DCVs.

Supplementary Material

Refer to Web version on PubMed Central for supplementary material.

Acknowledgments

The authors are indebted to Andy Fire, Yuji Kohara, Jeb Gaudet, Yo Suzuki, Bill Wood, and Janet Richmond for plasmids, strains and advice, and Paul Huber, Alena Kozlova and two anonymous reviewers for critical reading of this manuscript. This project was supported by NIH grant R01 GM82865, a UIC LAS Award for Faculty in the Natural Sciences, and State of Illinois funding to the Laboratory for Molecular Biology. Some strains were provided by the CGC, which is funded by NIH Office of Research Infrastructure Programs (P40 OD010440).

References

Albert PS, Riddle DL. Mutants of Caenorhabditis elegans that form dauer-like larvae. Dev Biol. 1988; 126:270–293. [PubMed: 3350212]

Albertson DG, Thomson JN. The pharynx of Caenorhabditis elegans. Philos Trans R Soc Lond B Biol Sci. 1976; 275:299–325. [PubMed: 8805]

Ardiel EL, Rankin CH. An elegant mind: learning and memory in Caenorhabditis elegans. Learn Mem. 2010; 17:191–201. [PubMed: 20335372]

Ashrafi K. Obesity and the regulation of fat metabolism. WormBook. 2007:1–20. [PubMed: 18050496]

Ausubel, FM. Current protocols in molecular biology. Greene Pub. Associates and Wiley-Interscience; J. Wiley, New York: 1990.

Avery L, Horvitz HR. Pharyngeal pumping continues after laser killing of the pharyngeal nervous system of C. elegans. Neuron. 1989; 3:473–485. [PubMed: 2642006]

Avery, L.; Thomas, JH. Feeding and Defecation. In: Riddle, DL.; Blumenthal, T.; Meyer, BJ.; Priess, JR., editors. C. elegans II. Cold Spring Harbor Laboratory Press; Cold Spring Harbor, NY: 1997. p. 679716

Avery L, You YJ. C. elegans feeding. WormBook. 2012:1–23. [PubMed: 22628186]

Berger MF, Philippakis AA, Qureshi AM, He FS, Estep PW 3rd, Bulyk ML. Compact, universal DNA microarrays to comprehensively determine transcription-factor binding site specificities. Nat Biotechnol. 2006; 24:1429–1435. [PubMed: 16998473]

Burdine RD, Branda CS, Stern MJ. EGL-17(FGF) expression coordinates the attraction of the migrating sex myoblasts with vulval induction in C. elegans. Development. 1998; 125:1083–1093. [PubMed: 9463355]

Burgoyne RD, Morgan A. Secretory granule exocytosis. Physiological reviews. 2003; 83:581–632. [PubMed: 12663867]

Fernandez AP, Gibbons J, Okkema PG. C. elegans peb-1 mutants exhibit pleiotropic defects in molting, feeding, and morphology. Dev Biol. 2004; 276:352–366. [PubMed: 15581870]

Ghai V, Gaudet J. The CSL transcription factor LAG-1 directly represses hlh-6 expression in C. elegans. Dev Biol. 2008; 322:334–344. [PubMed: 18706403]

Gumienny TL, Savage-Dunn C. TGF-beta signaling in C. elegans. WormBook. 2013:1–34. [PubMed: 23908056]

Hall DH, Hedgecock EM. Kinesin-related gene unc-104 is required for axonal transport of synaptic vesicles in C. elegans. Cell. 1991; 65:837–847. [PubMed: 1710172]

Harvey RP. NK-2 homeobox genes and heart development. Dev Biol. 1996; 178:203–216. [PubMed: 8812123]

Hobson RJ, Geng J, Gray AD, Komuniecki RW. SER-7b, a constitutively active Galphas coupled 5-HT7-like receptor expressed in the Caenorhabditis elegans M4 pharyngeal motorneuron. J Neurochem. 2003; 87:22–29. [PubMed: 12969249]

Hu PJ. Dauer. WormBook. 2007:1–19. [PubMed: 17988074]

Jia K, Albert PS, Riddle DL. DAF-9, a cytochrome P450 regulating C. elegans larval development and adult longevity. Development. 2002; 129:221–231. [PubMed: 11782415]

Kent WJ, Sugnet CW, Furey TS, Roskin KM, Pringle TH, Zahler AM, Haussler D. The human genome browser at UCSC. Genome Res. 2002; 12:996–1006. [PubMed: 12045153]

Krieglstein K, Unsicker K. Bovine chromaffin cells release a transforming growth factor-beta-like molecule contained within chromaffin granules. J Neurochem. 1995; 65:1423–1426. [PubMed: 7643124]

Krishna S, Maduzia LL, Padgett RW. Specificity of TGFbeta signaling is conferred by distinct type I receptors and their associated SMAD proteins in Caenorhabditis elegans. Development. 1999; 126:251–260. [PubMed: 9847239]

Lacmann A, Hess D, Gohla G, Roussa E, Krieglstein K. Activity-dependent release of transforming growth factor-beta in a neuronal network in vitro. Neuroscience. 2007; 150:647–657. [PubMed: 17997227]

Lewis, JA.; Fleming, JT. Basic Culture Methods, Methods in Cell Biology-Caenorhabditis elegans: Modern Biological Analysis of an Organism. Academic Press; San Diego, CA: 1995. p. 4-30.

Luo S, Kleemann GA, Ashraf JM, Shaw WM, Murphy CT. TGF-beta and insulin signaling regulate reproductive aging via oocyte and germline quality maintenance. Cell. 2010; 143:299–312. [PubMed: 20946987]

Marques G. Morphogens and synaptogenesis in Drosophila. J Neurobiol. 2005; 64:417–434. [PubMed: 16041756]

Mello, C.; Fire, A. DNA Transformation. In: Epstein, HF.; Shakes, DC., editors. Caenorhabditis elegans: Modern Biological Analysis of an Organism. Academic Press; San Diego, CA: 1995. p. 451-482.

Minoo P, Su G, Drum H, Bringas P, Kimura S. Defects in tracheoesophageal and lung morphogenesis in Nkx2.1(-/-) mouse embryos. Dev Biol. 1999; 209:60–71. [PubMed: 10208743]

Morita K, Chow KL, Ueno N. Regulation of body length and male tail ray pattern formation of Caenorhabditis elegans by a member of TGF-beta family. Development. 1999; 126:1337–1347. [PubMed: 10021351]

Mu Y, Gudey SK, Landstrom M. Non-Smad signaling pathways. Cell Tissue Res. 2012; 347:11–20. [PubMed: 21701805]

Nonet ML. Visualization of synaptic specializations in live C. elegans with synaptic vesicle protein-GFP fusions. J Neurosci Methods. 1999; 89:33–40. [PubMed: 10476681]

Okkema PG, Fire A. The Caenorhabditis elegans NK-2 class homeoprotein CEH-22 is involved in combinatorial activation of gene expression in pharyngeal muscle. Development. 1994; 120:2175–2186. [PubMed: 7925019]

Pocock R, Hobert O. Hypoxia activates a latent circuit for processing gustatory information in C. elegans. Nat Neurosci. 2010; 13:610–614. [PubMed: 20400959]

Pradhan L, Genis C, Scone P, Weinberg EO, Kasahara H, Nam HJ. Crystal structure of the human NKX2.5 homeodomain in complex with DNA target. Biochemistry. 2012; 51:6312–6319. [PubMed: 22849347]

Raharjo WH, Ghai V, Dineen A, Bastiani M, Gaudet J. Cell architecture: surrounding muscle cells shape gland cell morphology in the Caenorhabditis elegans pharynx. Genetics. 2011; 189:885–897. [PubMed: 21868609]

Ray P, Schnabel R, Okkema PG. Behavioral and synaptic defects in C. elegans lacking the NK-2 homeobox gene ceh-28. Dev Neurobiol. 2008; 68:421–433. [PubMed: 18161854]

Roberts AF, Gumienny TL, Gleason RJ, Wang H, Padgett RW. Regulation of genes affecting body size and innate immunity by the DBL-1/BMP-like pathway in Caenorhabditis elegans. BMC Dev Biol. 2010; 10:61. [PubMed: 20529267]

Savage C, Das P, Finelli AL, Townsend SR, Sun CY, Baird SE, Padgett RW. Caenorhabditis elegans genes sma-2, sma-3, and sma-4 define a conserved family of transforming growth factor beta pathway components. Proc Natl Acad Sci U S A. 1996; 93:790–794. [PubMed: 8570636]

Schafer WR. Deciphering the neural and molecular mechanisms of C. elegans behavior. Curr Biol. 2005; 15:R723–729. [PubMed: 16139205]

Sieber C, Kopf J, Hiepen C, Knaus P. Recent advances in BMP receptor signaling. Cytokine Growth Factor Rev. 2009; 20:343–355. [PubMed: 19897402]

Sieburth D, Madison JM, Kaplan JM. PKC-1 regulates secretion of neuropeptides. Nat Neurosci. 2007; 10:49–57. [PubMed: 17128266]

Smit RB, Schnabel R, Gaudet J. The HLH-6 transcription factor regulates C. elegans pharyngeal gland development and function. PLoS Genet. 2008; 4:e1000222. [PubMed: 18927627]

Specht H, Peterziel H, Bajohrs M, Gerdes HH, Krieglstein K, Unsicker K. Transforming growth factor beta2 is released from PC12 cells via the regulated pathway of secretion. Mol Cell Neurosci. 2003; 22:75–86. [PubMed: 12595240]

Speese S, Petrie M, Schuske K, Ailion M, Ann K, Iwasaki K, Jorgensen EM, Martin TF. UNC-31 (CAPS) is required for dense-core vesicle but not synaptic vesicle exocytosis in Caenorhabditis elegans. J Neurosci. 2007; 27:6150–6162. [PubMed: 17553987]

Suzuki Y, Yandell MD, Roy PJ, Krishna S, Savage-Dunn C, Ross RM, Padgett RW, Wood WB. A BMP homolog acts as a dose-dependent regulator of body size and male tail patterning in Caenorhabditis elegans. Development. 1999; 126:241–250. [PubMed: 9847238]

Weaver M, Yingling JM, Dunn NR, Bellusci S, Hogan BL. Bmp signaling regulates proximal-distal differentiation of endoderm in mouse lung development. Development. 1999; 126:4005–4015. [PubMed: 10457010]

White JG, Southgate E, Thomson JN, Brenner S. The Structure of the Nervous System of the Nematode Caenorhabditis elegans. Philosophical Transactions of the Royal Society of London. B, Biological Sciences. 1986; 314:1–340.

Yoshida S, Morita K, Mochii M, Ueno N. Hypodermal expression of Caenorhabditis elegans TGF-beta type I receptor SMA-6 is essential for the growth and maintenance of body length. Dev Biol. 2001; 240:32–45. [PubMed: 11784045]

Zhang X, Zhang Y. DBL-1, a TGF-beta, is essential for Caenorhabditis elegans aversive olfactory learning. Proc Natl Acad Sci U S A. 2012; 109:17081–17086. [PubMed: 23019581]

Zhang YE. Non-Smad pathways in TGF-beta signaling. Cell research. 2009; 19:128–139. [PubMed: 19114990]

Zhu NL, Li C, Xiao J, Minoo P. NKX2.1 regulates transcription of the gene for human bone morphogenetic protein-4 in lung epithelial cells. Gene. 2004; 327:25–36. [PubMed: 14960358]

Zugasti O, Ewbank JJ. Neuroimmune regulation of antimicrobial peptide expression by a noncanonical TGF-beta signaling pathway in Caenorhabditis elegans epidermis. Nature immunology. 2009; 10:249–256. [PubMed: 19198592]

Highlights

- The NK-2 homeodomain factor CEH-28 activates expression of *dbl-1* in the M4 neuron
- CEH-28 directly targets a cell-specific transcriptional enhancer in *dbl-1*
- DBL-1 secretion from M4 affects morphology of the nearby pharyngeal g1 gland cells
- The DBL-1 signals affecting gland cells do not depend on R-Smads
- This work reveals a novel neuroendocrine function for M4

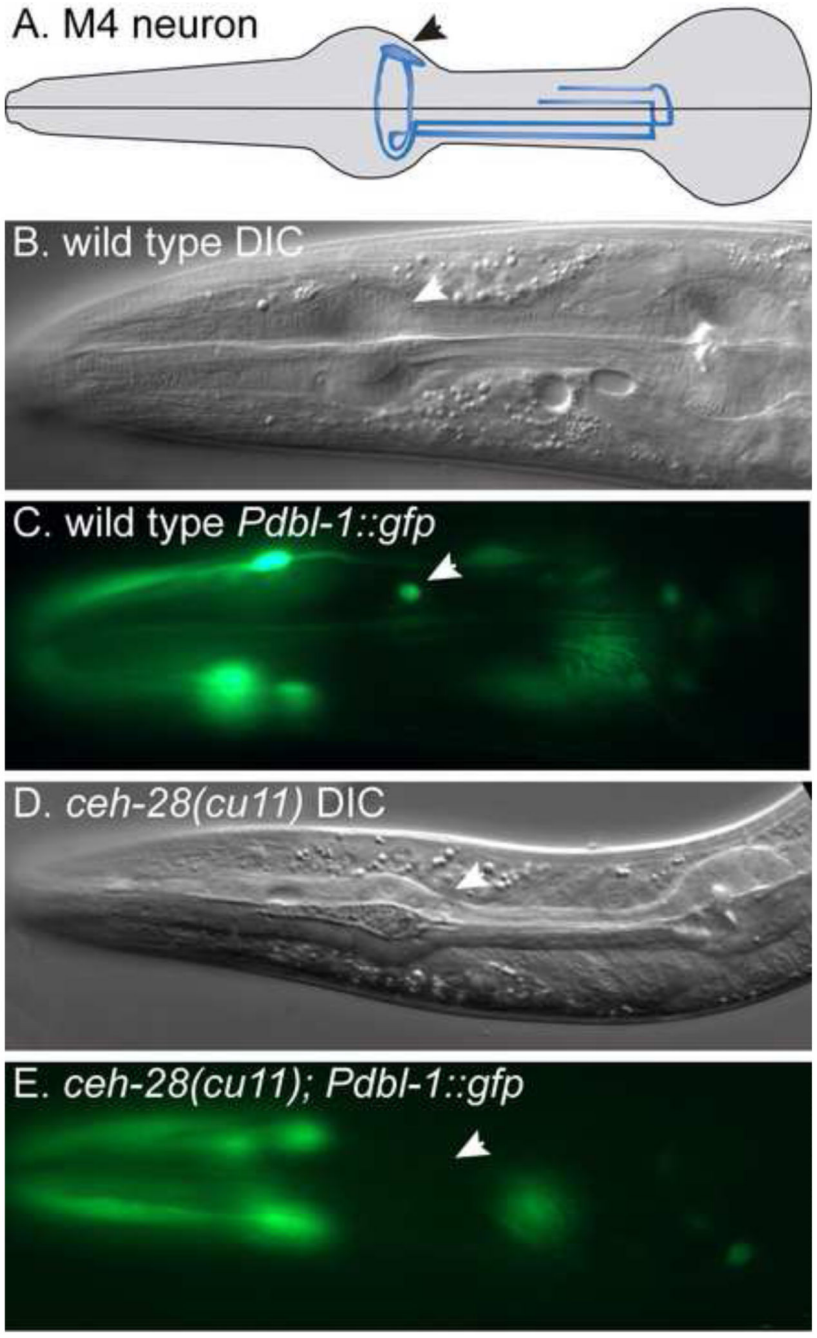

Figure 1. *Pdbl-1::gfp* expression in wild type and *ceh-28* mutants

(A) Schematic diagram of the pharynx indicating the M4 neuron (blue) (adapted from Albertson and Thompson, 1976). The M4 cell body (arrowhead) is located in the pharyngeal metacorpus, and it extends two processes through the pharyngeal isthmus. (B-E) DIC and fluorescence micrographs of a wild-type animal (B, C) and a *ceh-28(cu11)* mutant (D, E) expressing *Pdbl-1::gfp*. The M4 neuron is marked (arrowheads).

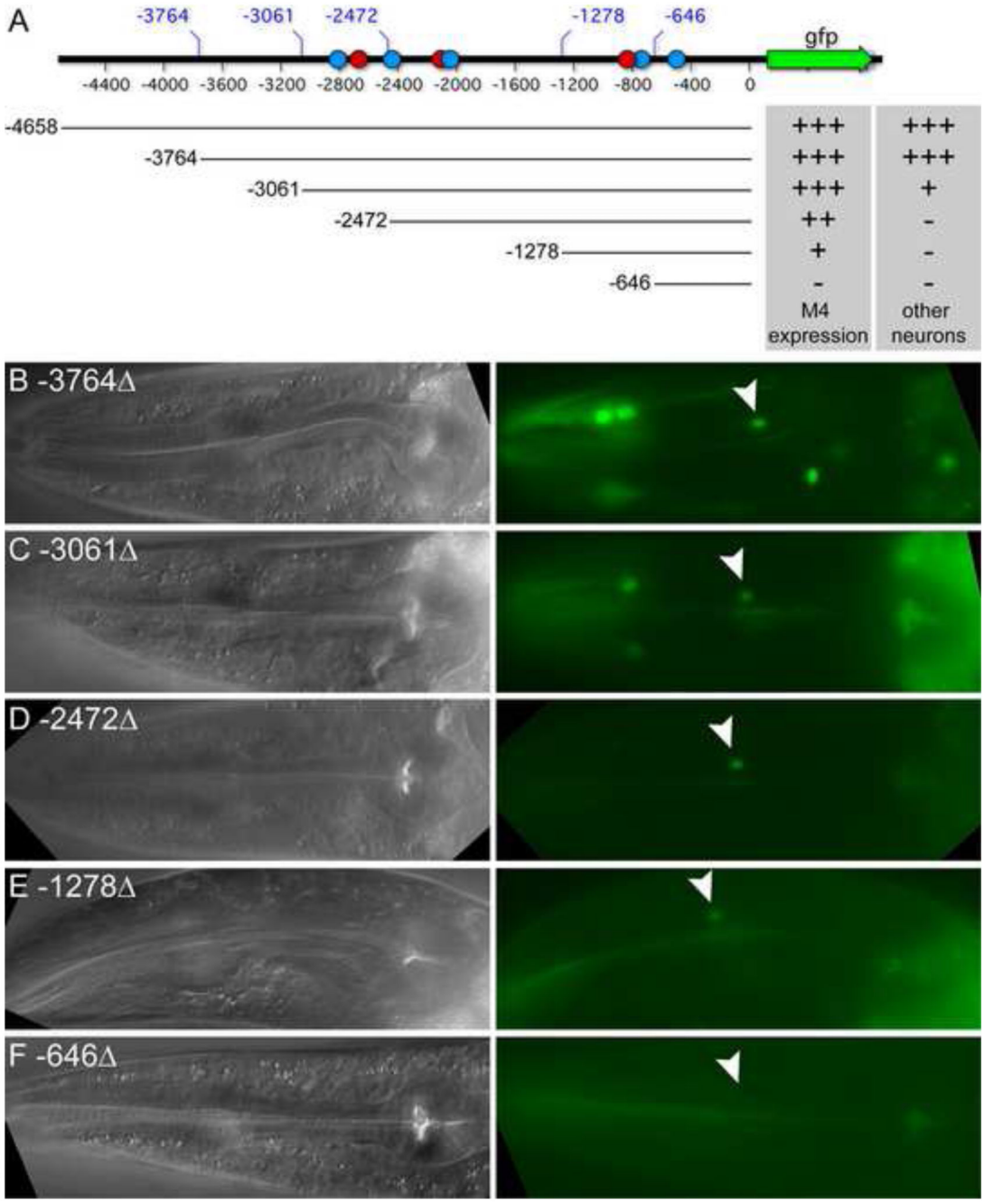

Figure 2. Deletion analysis of the *dbl-1* promoter

(A) Schematic diagram of the *Pdbl-1::gfp* indicating candidate CEH-28 binding sites (circles; red indicate conserved) and the endpoints of promoter deletions. Relative expression levels and frequency in M4 and other neurons inside and outside the pharynx are indicated. Deletion endpoints are numbered by distance upstream of the *dbl-1* ATG codon. (B-F) DIC (left) and fluorescence (right) micrographs of adult animals expressing the indicated *Pdbl-1::gfp* deletions numbered as in (A). The M4 cell body is marked with an arrowhead.

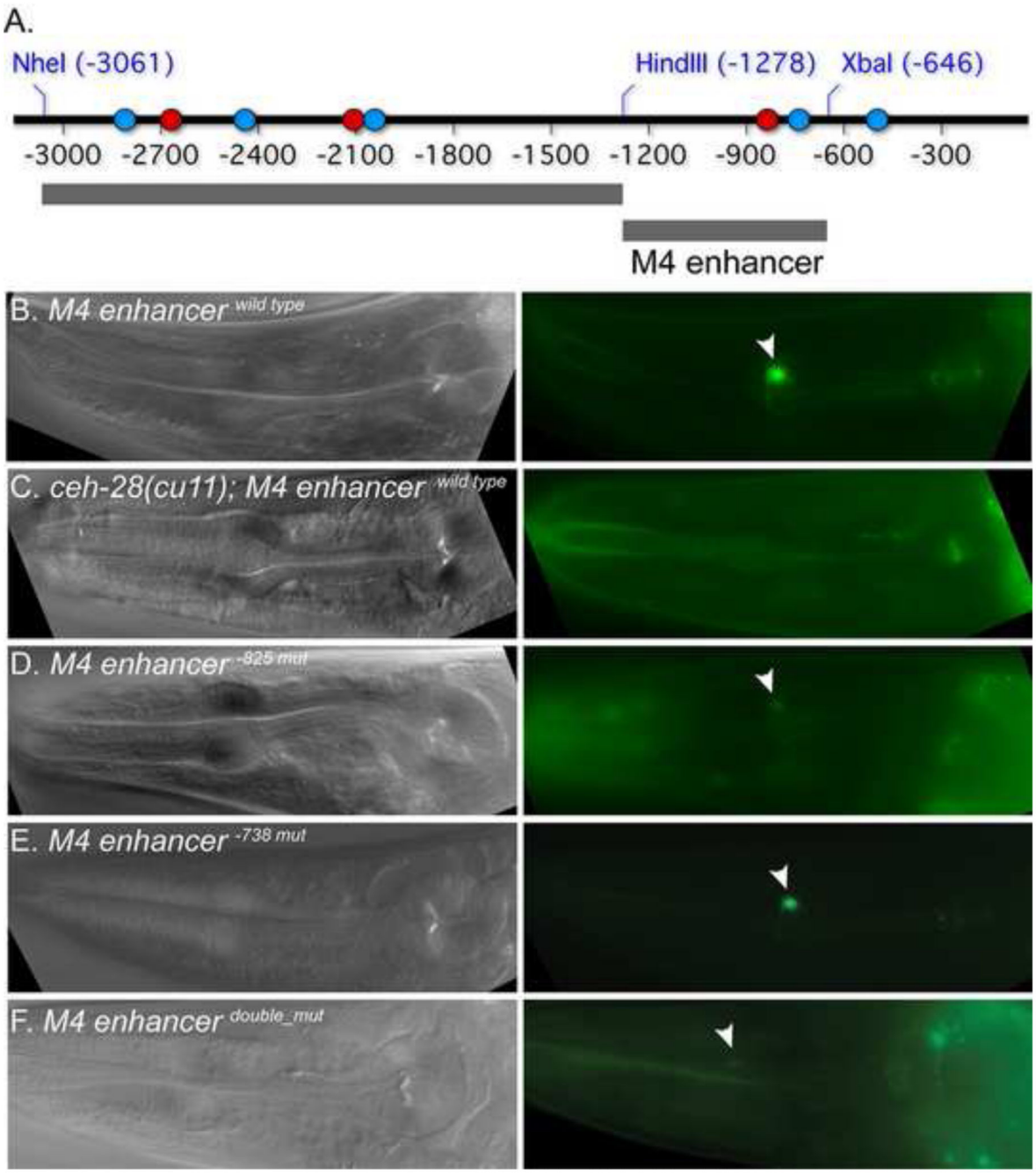

Figure 3. Identification and analysis of the M4 enhancer

(A) Schematic diagram of the *dbl-1* promoter region and fragments tested for enhancer activity (gray bars; numbered as in Figure 1). (B, C) DIC and fluorescence micrographs of wild-type (B) and *ceh-28(cu11)* (C) adult animals expressing Δ*pes-10::gfp* containing the wild-type M4 enhancer. (D-E) Micrographs of wild-type adults expressing Δ*pes-10::gfp* containing mutated M4 enhancers. The M4 cell body is marked with an arrowhead.

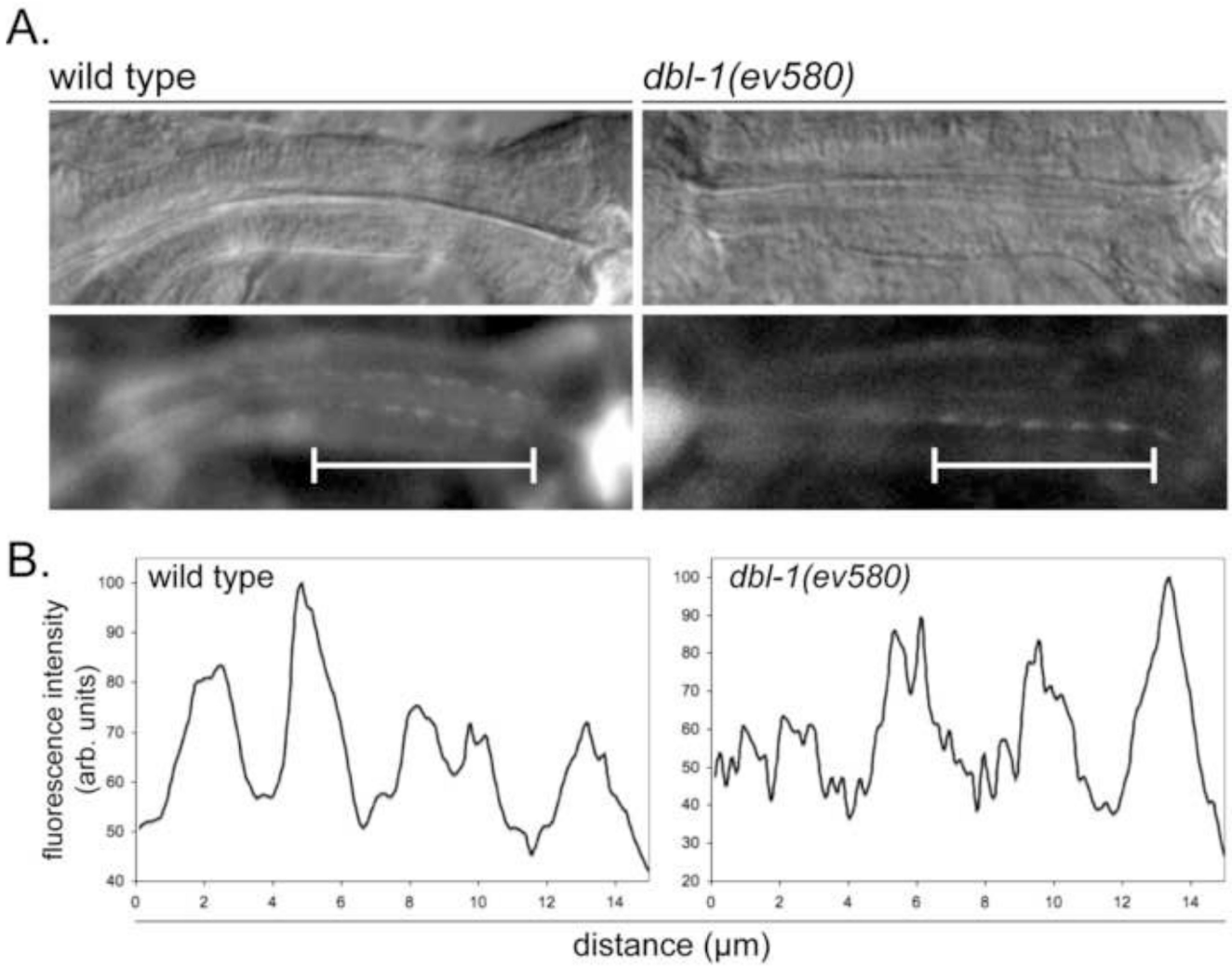

Figure 4. Characterization of SNB-1::GFP marked synapses in *dbl-1* mutants

(A) DIC and Fluorescence micrographs showing the pharyngeal isthmus of wild-type and *dbl-1(ev580)* mutant adults expressing SNB-1::GFP. M4 synapses appear as fluorescent dashes in the M4 processes in the posterior half of the isthmus (bar). Anterior is left. Two processes are visible in wild type while a single process is visible in *dbl-1(ev580)*. (B) Representative profiles of SNB-1::GFP fluorescence intensity in M4 processes.

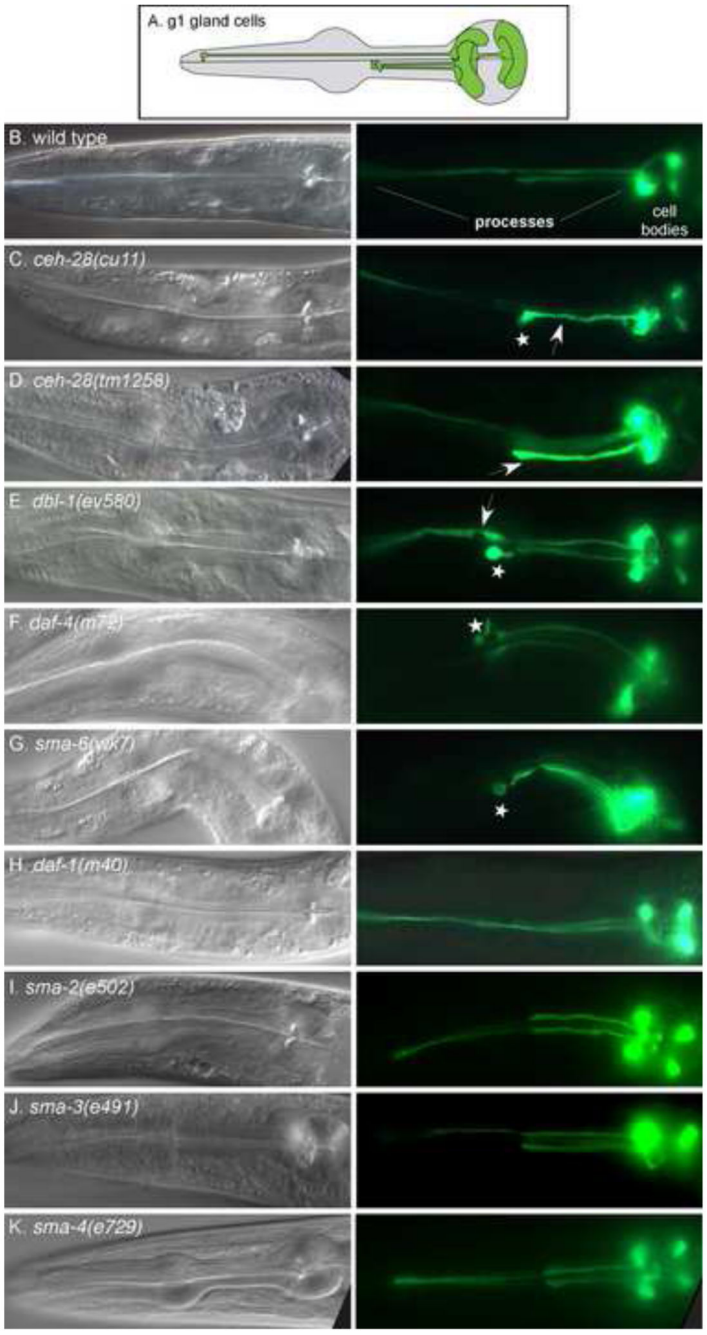

Figure 5. g1 gland cell defects in *ceh-28* and TGF-ß signaling mutants

(A) Schematic diagram of the pharynx indicating the g1 gland cells (green) (adapted from (Albertson and Thomson, 1976)). (B-K) DIC and fluorescence micrographs of the indicated mutants expressing the g1 gland cell markers *phat-3::yfp* (B-H) or *phat-1::yfp* (I-K). In wild-type animals, the gland cell processes are thin and a uniform diameter. Thickened processes (arrowheads) and abnormal swellings (stars) are indicated. In some cases only the subventral process are in focus.

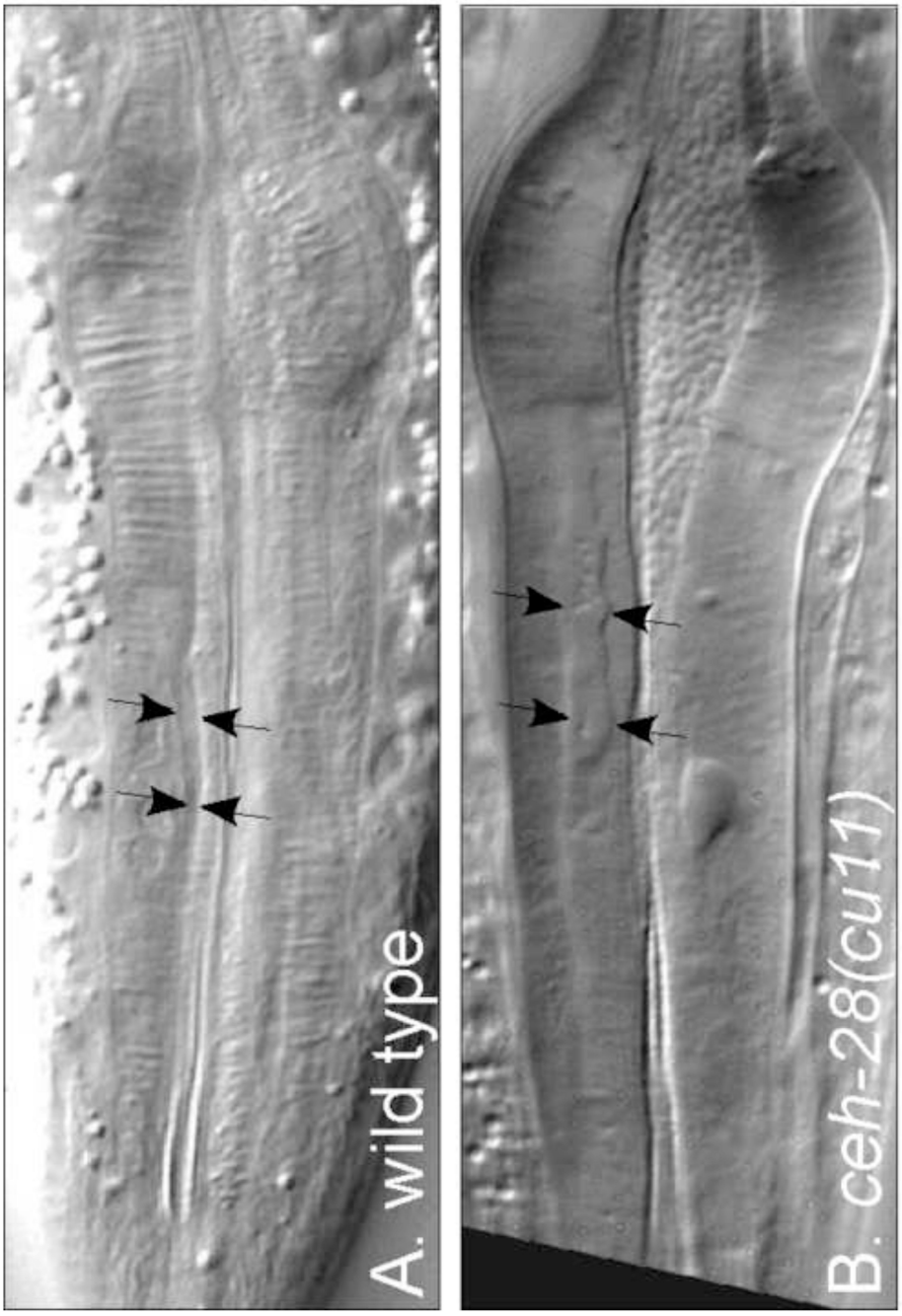

Figure 6. g1 gland cell defects in untransformed *ceh-28* mutants

DIC micrographs of the anterior pharynx with the width of the dorsal g1 gland cell process marked (arrows).

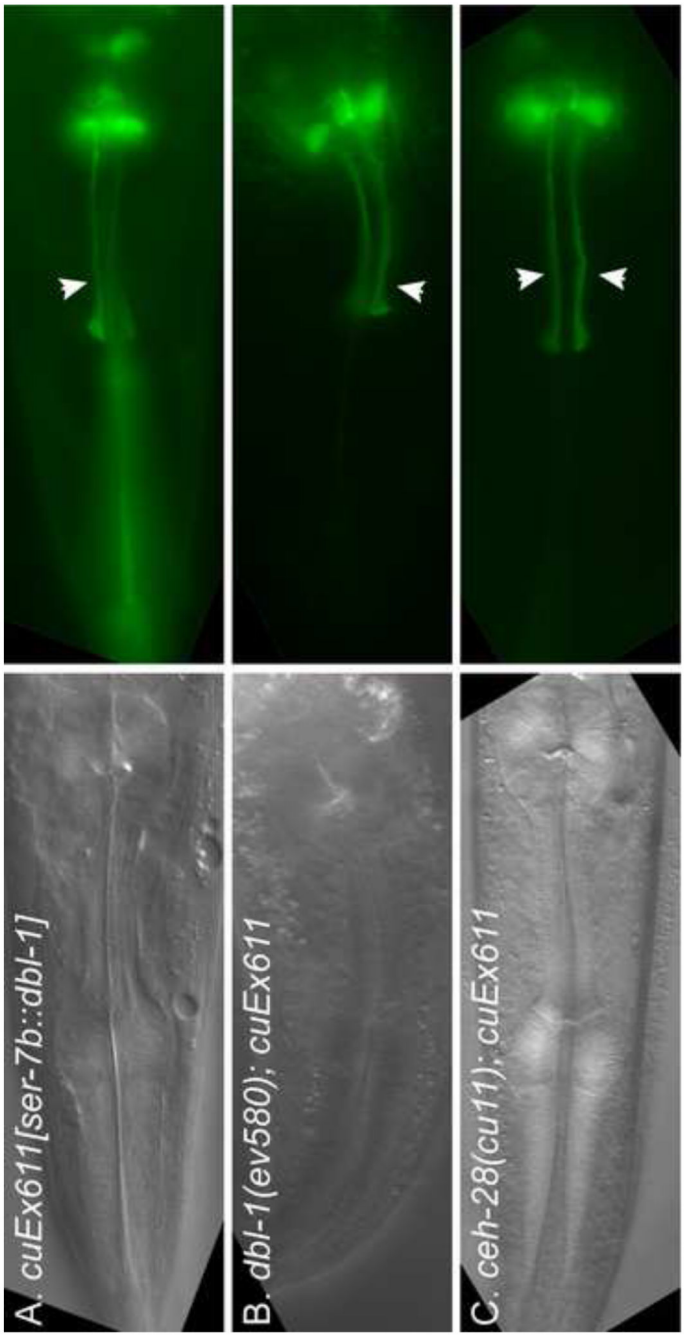

Figure 7. *dbl-1* expression in M4 rescues *dbl-1* and *ceh-28* mutant gland cell defects

DIC and fluorescence micrographs of animals of the indicated genotypes expressing *phat-3::yfp*in the g1 gland cells. Arrowhead mark in focus g1 processes.

Table 1

Frequency of *Pdbl-1::gfp* expression in M4

***Pdbl-1::gfp* promoter deletions**	**Frequency of expression in M4 (n)** [a]
−4658Δ	85% (40)
−2472Δ	64% (50)
−1278Δ	40% (45)
−646Δ	0% (40)

[a] M4 GFP expression was scored in transgenic adults

Table 2

Activity of the M4 enhancer depends on CEH-28 binding sites

genotype	Percent animals expressing GFP in M4 (n)[a]
cuEx613 [M4 enhancer$^{wild\ type}$]	100% (30)
ceh-28(cu11); cuEx613 [M4 enhancer$^{wild\ type}$]	0% (20)
cuEx619 [M4 enhancer$^{-825\ mut}$]	63% (30)
cuEx621 [M4 enhancer$^{-738\ mut}$]	95% (40)
cuEx627 [M4 enhancer^{double_mut}]	30% (37)

[a] transgenic adults were scored for GFP expression in M4

Table 3

Pharyngeal pumping and peristalsis in *dbl-1* mutants.

	Wild type[a]	*dbl-1(ev580)* [b]
Pump rate (pumps/min)	174 ± 39	179 ± 25
Procorpus contraction length (msec)	74 ± 14	79 ± 19
Posterior bulb contraction length (msec)	129 ± 28	118 ± 20
Isthmus peristalsis length (msec)	215 ± 38	210 ± 90
% pumps followed by isthmus peristalsis	2.5%	10.5%

[a] Five N2 L1s were recorded for 29-30 sec each, and a total of 442 pumps were analyzed.

[b] Five *dbl-1(ev580)* L1s were recorded for 20-30 sec each, and a total of 352 pumps were analyzed.

Table 4

Frequency of g1 gland cell abnormalities in *ceh-28* and TGF-ß signaling mutants.

Genotype	% adults exhibiting abnormal g1 gland cell processes (n)[a, b]
Wild type[c]	9 (98)
ceh-28(cu11) [c]	64 (22)
dbl-1(ev580) [c]	76 (50)
daf-4(m72) [c]	72 (36)
sma-6(wk7) [c]	68 (37)
daf-1(m40) [c]	25 (24)
sma-2(e502) [d]	8 (37)
sma-3(e491) [d]	10 (35)
sma-4(e729) [d]	30 (60)
daf-8(e1393) [d]	9 (43)
daf-14(dr77) [d]	10 (42)
daf-3(mg90) [c]	7 (28)
cuEx611[ser-7b::dbl-1 + phat-3::yfp] [e]	11 (38)
dbl-1(ev580); cuEx611 [e]	36 (68)
ceh-28(cu11); cuEx611 [e]	30 (20)

[a] g1 gland cell abnormalities include thick gland cell processes, or abnormal knobs or projections on the gland cell process.

[b] n = the total number of adult animals scored using the *yfp* reporters to visualize g1 gland cells

[c,d] gland cell morphology was scored using a *phat-3::yfp* transgene *ivEx[C49G7.4::YFP]* or a *phat-1::yfp* transgene *ivIs12* (d).

[e] *cuEx611* is an extrachromosomal transgene containing *phat-3::yfp* and *ser-7b::dbl-1*.